ASYMMETRIES MAKE THE DIFFERENCE: AN ANALYSIS OF TRANSISTOR-BASED ANALOG RING MODULATORS

Richard Hoffmann-Burchardi

Institut für Musikwissenschaft
Hochschule für Musik
Karlsruhe, Germany
hoffmann@hfm-karlsruhe.de

ABSTRACT

This work analyzes analog ring modulators based on bipolar transistors, such as the EMS VCS3 and the Doepfer A-114. It is shown that the perfectly symmetric standard model from literature [1][2] does not suffice to describe crucial first-order effects. A detailed analysis of the circuit using mismatched parts is performed. The insights gained from this analysis are used to formulate a digital model which can be easily implemented and which captures the essential audible effects.

1. INTRODUCTION

Ring modulators comprise an essential audio effect, and have been used both in commercial as well as in avantgarde music, in particular by Stockhausen — one of his most famous works, 'Mantra', uses two pianos, each processed by a ring modulator [3].

Ring modulation is equivalent to the multiplication of two signals, called carrier and modulator, in the time domain (Fig. 1).

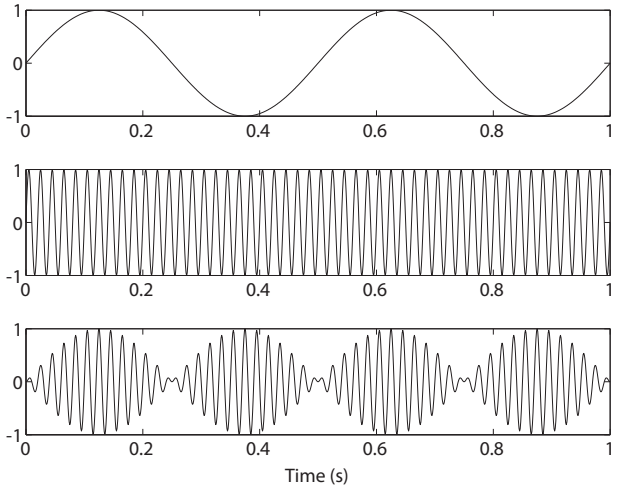

Figure 1: *Ring modulation of two sinusoids, 2 Hz and 50 Hz.*

In the frequency domain, the sums and differences of the two signals' frequencies appear, which follows from the trigonometric identity

$$sin(f_x)sin(f_y) = \frac{1}{2}(cos(f_x + f_y) - cos(f_x - f_y)) \quad (1)$$

with the carrier frequency f_x and the modulator frequency f_y.

Analog ring modulators can be classified into active and passive topologies [4]. The most common passive design is based on four diodes aligned in a ring (hence the term ring modulator) and two transformers; its working principle, as well as a possible digital model, has been covered in [5]. In this paper, a common active topology used for ring modulation is studied, which is based on bipolar transistors. This design can be found in the EMS VCS3 and Doepfer A-114 ring modulators. The VCS3 contains the circuit in discrete form, while the A-114 works IC-based.

This article comprises three sections. The first section describes the working principle of a transistor-based four quadrant analog multiplier as covered in literature, assuming perfectly matched parts. The second section studies the effects that occur due to network asymmetries, which can be observed in real-world ring modulators and are perceptually relevant. The last section proposes a digital implementation approximating such imbalance effects.

2. DESCRIPTION AND ANALYSIS OF THE TRANSISTOR-BASED RING MODULATOR

A simple analog multiplication can be performed with a differential amplifier, consisting of two bipolar transistors, Q1 and Q2 (Fig. 2). A differential voltage v_x is applied at the bases of both transistors, the emitters are coupled and connected to a current source I_0. The output currents I_{C1} and I_{C2} are related to the differential input voltage v_x and the current I_0 at the emitters by [1]

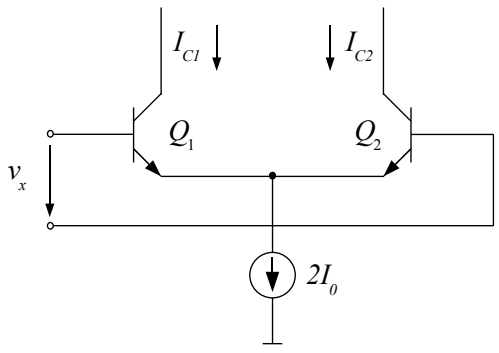

Figure 2: *Differential amplifier.*

$$I_{C1} = \frac{2I_0}{1+exp(-\frac{v_x}{V_t})} = -I_0 tanh(\frac{-v_x}{2V_t}) + I_0 \quad (2)$$

$$I_{C2} = \frac{2I_0}{1+exp(\frac{v_x}{V_t})} = -I_0 tanh(\frac{v_x}{2V_t}) + I_0 \quad (3)$$

neglecting the base current. V_t is the so-called thermal voltage, approximately 26mV at 25°C. The difference current

$$\Delta I = I_{C1} - I_{C2} = 2I_0 tanh(\frac{v_x}{2V_t}) \quad (4)$$

is about proportional to I_0 and v_x for small values of v_x.

Replacing the current source I_0 by additional circuitry, it is possible to apply a second input signal. The transistors Q1 and Q2, however, require the input current to be positive, and, therefore, such a circuit would result in only a two-quadrant multiplier not suitable for ring modulation.

A four-quadrant multiplier based on transistors was proposed by Gilbert [6] and is shown in Fig. 3. The circuit is based on three differential amplifiers: One emitter-coupled tranistor pair Q5/Q6 is connected in series with two cross-coupled transistor pairs Q1/Q2 and Q3/Q4.

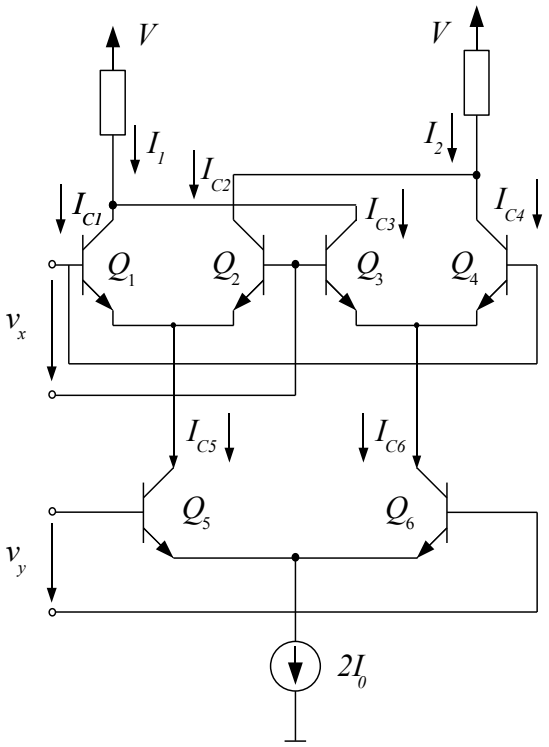

Figure 3: *Gilbert four-quadrant multiplier.*

The bottom differential amplifier multiplies the current $2I_0$ with the modulator signal v_y in the same manner as discussed above, generating the currents

$$I_{C5} = I_0 tanh(\frac{v_y}{2V_t}) + I_0 \quad (5)$$

$$I_{C6} = -I_0 tanh(\frac{v_y}{2V_t}) + I_0 \quad (6)$$

at the collectors of Q5 and Q6. Both currents are multiplied again, resulting in the currents [2]

$$I_{C1} = \frac{I_{C5}}{2} tanh(\frac{v_x}{2V_t}) + \frac{I_{C5}}{2} \quad (7)$$

$$I_{C2} = -\frac{I_{C5}}{2} tanh(\frac{v_x}{2V_t}) + \frac{I_{C5}}{2} \quad (8)$$

$$I_{C3} = -\frac{I_{C6}}{2} tanh(\frac{v_x}{2V_t}) + \frac{I_{C6}}{2} \quad (9)$$

$$I_{C4} = \frac{I_{C6}}{2} tanh(\frac{v_x}{2V_t}) + \frac{I_{C6}}{2} \quad (10)$$

The currents are added at the collectors Q1/Q3 and Q2/Q4, yielding the output currents:

$$I_1 = I_{C1} + I_{C3} = I_0 tanh(\frac{v_y}{2V_t}) tanh(\frac{v_x}{2V_t}) + I_0 \quad (11)$$

$$I_2 = I_{C2} + I_{C4} = -I_0 tanh(\frac{v_y}{2V_t}) tanh(\frac{v_x}{2V_t}) + I_0 \quad (12)$$

It is obvious that the output currents are a product of both input signals. The constant current I_0 can be removed in a later stage and is thus irrelevant. Since linearizing resistors are used at the emitters of the transistors Q5 and Q6 in practical circuits, the approximation tanh(x) ≈ x may be used for the modulator input signal. The resulting output signal can then be described by

$$o(t) = y(t) tanh(x(t)) \quad (13)$$

with the carrier signal $x(t)$ and the modulator signal $y(t)$.

3. EFFECTS CAUSED BY CIRCUIT ASYMMETRIES

3.1. Comparison of an analog ring modulator and the idealized model

In the previous section, it was shown that the output of the Gilbert multiplier circuit can be described by equation 13, assuming perfectly identical transistors. Measurements on the Doepfer ring modulator, which is based on the Gilbert network, were performed to evaluate this model. Applying a sinusoid of 1 kHz at the carrier input and a sinusoid of 100 Hz at the modulator input, then performing a spectral analysis of the recorded output yields Fig. 4. Using the approximation in Eq. 13, the peaks would be expected at the frequencies

$$f_x \pm f_y, 3f_x \pm f_y, 5f_x \pm f_y, ... \quad (14)$$

with f_x being the carrier and f_y being the modulator frequency. The odd order harmonics are introduced by the tanh() function:

$$tanh(x) = x - \frac{x^3}{3} + \frac{2x^5}{15} - ... \quad (15)$$

Additional spectral components appear in the figure, however, in particular f_x, f_y, $2f_x$ and $2f_y$. The next sections will show that these output components can be explained by mismatched parts.

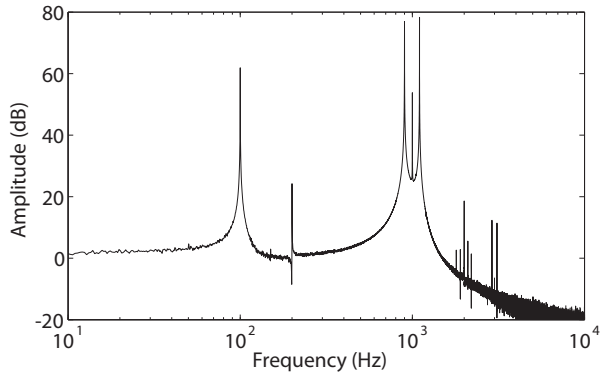

Figure 4: *Fourier analysis of the Doepfer A-114 ring modulator, applying two sinusoids of 100 Hz and 1 kHz.*

3.2. Asymmetries in the modulator input stage

In a perfectly balanced state, the current $2I_0$ is split evenly between the two transistors Q5 and Q6. In reality, however, the current will mix slightly differently with the modulator current at the collectors of the transistors, resulting in a DC offset. This effect can be modelled by adding a constant current ΔI to one collector and subtracting it from the other one:

$$I_{C5} = I_0 tanh(\frac{v_y}{2V_t}) + I_0 + \Delta I \quad (16)$$

$$I_{C6} = -I_0 tanh(\frac{v_y}{2V_t}) + I_0 - \Delta I \quad (17)$$

Repeating the calculations performed in Eq. 7-10, the output currents are:

$$I_1 = I_0 tanh(\frac{v_y}{2V_t}) tanh(\frac{v_x}{2V_t}) + I_0 + \Delta I tanh(\frac{v_x}{2V_t}) \quad (18)$$

$$I_2 = -I_0 tanh(\frac{v_y}{2V_t}) tanh(\frac{v_x}{2V_t}) + I_0 - \Delta I tanh(\frac{v_x}{2V_t}) \quad (19)$$

Comparing these equations to the ideal case of perfectly matched transistors, it can be seen that a portion of the carrier input v_x always leaks through to the output, even in the absence of a modulator signal.

3.3. Asymmetries in the carrier input stage

The four transistors Q1-Q4, multiplying the carrier input v_x and the differential modulator currents I_{C5} and I_{C6}, will not be fully symmetric in practice. Analyzing this effect is more difficult than in the preceeding section, as imbalances in the transistors Q1-Q4 will affect both the output signal as well as the modulator stage [7]. Hence, a MultiSim analysis of the circuit using six BC550 transistor models is performed instead. The transistors are assigned slightly different values for the saturation current I_s. Setting the modulator signal to 0V, while applying a sinusodial signal to the carrier input, exhibits a leakage effect — the sinusodial carrier signal leaks through to collectors Q5 and Q6, thus causing the signal to be multiplied with itself. Feeding two sinusodial signals of 1 kHz and 100 Hz into the carrier and modulator inputs, respectively, and performing a Fourier analysis of the output results in the spectrum shown in Fig. 5. The expected multiplication result is the sum and difference frequencies of both sinusoids, 1 kHz $\pm$ 100 Hz = 1100 Hz and 900 Hz, which are the dominant peaks in the figure. The third largest peak is at 2 kHz, showing that the carrier signal has been multiplied with itself. Additionally, it can be seen that both the modulator and carrier leak through to the output (peaks at 1 kHz and 100 Hz, which were the input frequencies).

Soundwise, this result is interesting if the signal applied to the carrier input is a broadband signal. In that case, many even order harmonics will appear at the output, which may increase the perceived sound quality at least for some input signals [8].

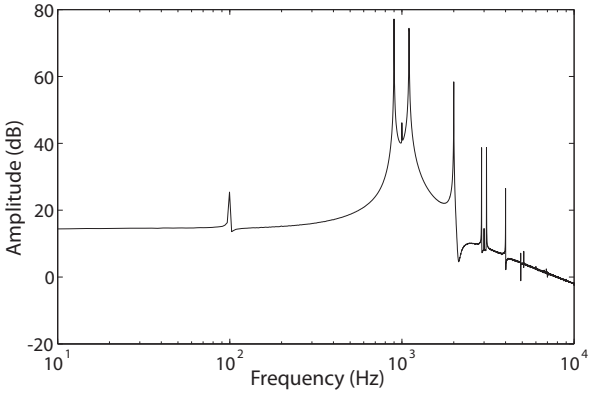

Figure 5: *MultiSim fourier analysis of an imbalanced multiplier circuit using 100 Hz and 1 kHz sinusoids as inputs.*

3.4. Summary of asymmetry effects

By considering the results of the previous paragraphs, the dominant peaks at 1000 Hz $\pm$ 100 Hz, 3000 Hz $\pm$ 100 Hz as well as 100, 1000 and 2000 Hz in Fig. 4 can be explained by the asymmetries and nonlinearities of the transistor stages. There is, however, also a strong peak at 200 Hz. This peak indicates that the ideal current source $2I_0$ used in the model is not sufficiently accurate to simulate the behavior of the circuit. Apparently, leakage and thus self-modulation occurs in the modulator input stage as well. A more detailed model, replacing the current source by the actual circuitry used, would be required to analyze these effects in further detail.

Designers of the EMS VCS3 ring modulator try to overcome the leakage problems by adding a portion of the carrier signal to the modulator input and vice versa, which can be seen from the schematic in [9]. The MC1496 multiplier chip used in the Doepfer A-114 ring modulator module relies on outside circuitry to balance part tolerances, as the example circuits in the datasheet show [10]. In practice, however, both ring modulators exhibit audible leakage effects.

4. DIGITAL MODEL

Using the insights from the previous section, a discrete-time model may be realized. The dominant peaks in the spectrum produced by the analog ring modulator can be implemented by adding a portion

of the carrier and modulator inputs to the output, as well as adding a fraction of the modulator to the carrier input and vice versa, thus yielding the equation:

$$\begin{aligned} o(n) &= (y(n) + a_1 x(n)) tanh(x(n) + a_2 y(n)) \\ &\quad + a_3 x(n) + a_4 y(n) \end{aligned} \tag{20}$$

The carrier signal x(n) and the modulator signal y(n) are given in discrete time, for the coefficients holds

$$0 < a_{1,2,3,4} \ll 1$$

Applying two sinusoids of 100 Hz and 1 kHz with an amplitude of 0.25 each and setting $a_1 = a_2 = a_3 = a_4 = 0.01$ yields the spectrum shown in Fig. 6. Comparing this result to Fig. 4, it can be seen that the dominant spectral components occurring in the analog ring modulator are well approximated by this model. Not covered are various sidebands of lower magnitude, most notably around 2 kHz. Those sidebands are a product of the even order carrier component at 2 kHz and the modulator components at 100 and 200 Hz.

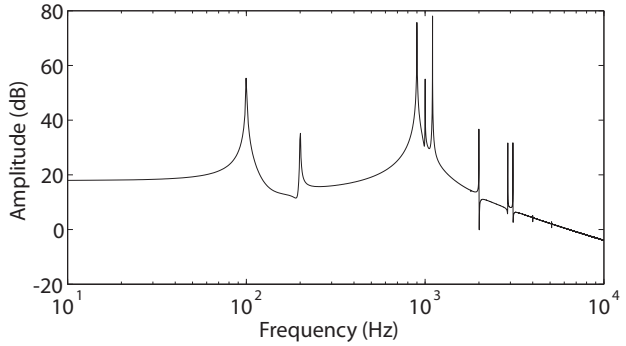

Figure 6: *Fourier analysis of the digital model using 1 kHz and 100 Hz sinusoids as inputs.*

Since the multiplication of two signals produces the sums and differences of all frequency components present in the signals, a digital implementation of a ring modulator should use an oversampling factor of 2 to prevent aliasing noise. The tanh() function used on the carrier input will add an infinite amount of odd order harmonics, which will require higher oversampling factors to reduce aliasing if high carrier levels are used. Another possible method is to approximate the tanh() function by a bandlimited polynomial and use individual anti-aliasing filters for each degree of the polynomial, thereby avoiding the need for additional oversampling [11].

5. CONCLUSIONS AND FUTURE WORK

This work has presented an analysis of transistor-based analog ring modulators. It was shown that network asymmetries as well as nonlinearities are the primary reasons for the particular sound of such devices. A simple digital model has been proposed, which is easy to implement and which captures the essential effects. A more sophisticated model could relate the parameters directly to circuit elements and add dynamic behavior, for instance based on subtle temperature changes. Furthermore, future work could investigate the impact of asymmetries in other audio effect circuits.

6. ACKNOWLEDGMENTS

The author would like to express his gratitude to Prof. Dr. Thomas Troge, Dr. Christian Rode and Jouni Airaksinen for their support and valuable comments on this article.

7. REFERENCES

[1] P. R. Gray and R. G. Meyer, *Analysis and Design of Analog Integrated Circuits*, chapter 10, p. 668, John Wiley and Sons, New York, 1977.

[2] U. Tietze, Ch. Schenk, and E. Gamm, *Electronic Circuits*, chapter 28, p. 1419, Springer, Heidelberg, 2008.

[3] K. Stockhausen, *Introduction to Mantra*, Stockhausen Verlag, Kuerten, Germany, 2003.

[4] F. Ellinger, *Radio Frequency Integrated Circuits and Technologies*, chapter 10, pp. 359–385, Springer, Heidelberg, Germany, 2007.

[5] R. Hoffmann-Burchardi, "Digital simulation of the diode ring modulator for musical applications," in *Proc. Digital Audio Effects (DAFx-08)*, Helsinki, Finland, Sept. 1-4, 2008, pp. 165–168.

[6] B. Gilbert, "A precise four-quadrant multiplier with subnanosecond response," *IEEE Journal of Solid-State Circuits*, vol. 3, no. 4, pp. 365–373, Dec. 1968.

[7] C. Toumazou and G. Moschytz, *Trade-Offs in Analog Circuit Design*, chapter 27, pp. 812–813, Kluwer Academic Publishing, Boston, 2002.

[8] R. O. Hamm, "Tubes versus transistors - is there an audible difference?," *J. Audio Eng. Soc.*, vol. 21, no. 4, pp. 267–273, May 1973.

[9] M. Urekar, "VCS3 Type Ring Modulator," Available at http://members.tripod.com/urekarm/synth/vcs3_rm.pdf, accessed March 31, 2009.

[10] OnSemi, "MC1496 Balanced Modulator," Available at http://www.onsemi.com/pub_link/Collateral/MC1496-D.PDF, accessed April 2, 2009.

[11] J. Schattschneider and U. Zölzer, "Discrete-time models for nonlinear audio systems," in *Proc. Digital Audio Effects (DAFx-99)*, Trondheim, Norway, Dec., 1999, pp. 45–48.